Chapter 1

INTRODUCTION

1.1 Introduction to Liquefaction

Liquefaction is a devastating instability associated with saturated, loose, and cohesionless soils. It is typically associated with earthquake-induced shaking that causes the ground to lose its bearing strength and act like a fluid. This can cause entire buildings to topple and cars to get sucked in. It can cause surface layers to slide downhill, damaging roads and rupturing distributed infrastructure systems like water and gas lines. It can also cause floatation, whereby objects buried underground such as pipelines and manhole covers float up to the surface. The 1964 earthquake in Niigata, Japan and the 2010-11 earthquake sequence in Christchurch, New Zealand provide prime examples of earthquake-induced liquefaction failures.

Although primarily associated with earthquakes, liquefaction can also occur under static loading conditions [44]. Static liquefaction has been observed as a cause for failure of slopes in hydraulic fill dams, spoil tips, and tailings [8]. Examples include the 1966 Aberfan disaster, which resulted in the loss of 144 lives, and the failure of the Fort Peck Dam in 1936 that led to the loss of 80 lives. More recently, in November 2015, the failure of the Fundao dam in Brazil that resulted in the death of 19 people is also suspected to be caused by liquefaction [43].

Liquefaction is typically characterized by generation of excess pore pressure under undrained loading. The tendency of loose sands to densify under drained loading is well known [44]. When loose sands are saturated and loaded under undrained conditions, the tendency to densify causes an increase in pore pressure, leading to a decrease in effective confining pressure. This lowers the shear strength of the soil, causing it to liquefy. Based on the mechanism of deformation, liquefaction can be divided into flow liquefaction and cyclic mobility. Flow liquefaction can occur when the shear stress required for static equilibrium of a soil mass is greater than the shear strength of the soil in its liquefied state. It can occur under both static and cyclic loading. Once triggered, the soil experiences large deformations which may seem sudden and are catastrophic. Cyclic mobility, on the other hand, can occur

when the shear stress required for static equilibrium of a soil mass is less than the shear strength of soil. It can occur only under cyclic loading. In contrast with flow liquefaction, cyclic mobility causes deformations to develop incrementally during an earthquake, and can lead to large permanent deformations that are termed 'lateral spreading' [44]. Chapter 3 discusses these mechanisms in greater detail.

1.2 Evaluation of liquefaction susceptibility

In order to mitigate the effects of liquefaction, it is important to be able to evaluate liquefaction susceptibility of a soil. This evaluation essentially consists of determining two kinds of stresses:

(a) Stresses imposed on the soil by external loading.

(b) Stresses needed to liquefy the soil.

If (a) $\geq$ (b), soil liquefies, else it is stable. Evaluation of stresses in (a) is based on a knowledge and estimation of field conditions. For instance, in the case of static slope stability analyses, the angle of the slope can be used as a metric to estimate imposed stresses [32, 48]. In the case of earthquake-induced loading, the so-called 'simplified procedure' is commonly used [34, 71, 88].

Evaluation of stresses in (b) can be achieved via laboratory or in-situ testing of soils. For slope stability analyses in the case of spoil tips, tailings, and hydraulic-fill dams, estimating stresses needed for soil liquefaction is often done by obtaining a soil sample from the site, and subjecting it to static compression in a laboratory test [32, 48]. For earthquake-induced liquefaction assessments, recourse is often sought to in-situ tests such as standard penetration tests, cone penetration tests, and shear velocity measurements [34, 88]. In-situ tests are considered more representative of field behavior than laboratory testing, since retrieval of soil specimens from the field using typical drilling and sampling techniques induces a lot of disturbance, which destroys the existing mechanical structure. This makes it difficult to translate laboratory test results onto field conditions [34, 88]. However, interpretation of in-situ tests often relies on empirical correlations [34, 88], which inherently restricts the scope of their application.

To help with the flow of this thesis, the next few sub-sections provide a brief review of (i) the triaxial compression test, which is a common laboratory test, and (ii)

liquefaction charts, which are used to evaluate liquefaction resistance of soil to earthquakes. A review of these topics will help in motivating the research presented in this thesis.

(i) The Triaxial Compression Test

For slope stability analysis under static loading, estimating stresses needed for soil liquefaction is often done by subjecting a soil sample obtained from the site to static loading in a triaxial compression test [32, 48]. Subjecting a loose sand to triaxial compression under undrained loading causes it to liquefy; this is perhaps the simplest manifestation of liquefaction. The triaxial test involves using a cylindrical specimen, generally having a length/diameter ratio of 2, that is stressed under conditions of axial symmetry. Figure 1.1 shows a schematic of the test. A detailed description of the test setup can be found in a soil mechanics textbook [16, 85]. In essence, the soil specimen is confined in a rubber membrane, and is placed on a porous disc on a pedestal. There is a loading cap on top of the specimen that can impose an axial stress σ_a. The specimen is subjected to an all-round fluid pressure σ_r. There is also a provision for drainage of pore water through the pedestal that can also be used for measurement of pore water pressure if drainage is prevented.

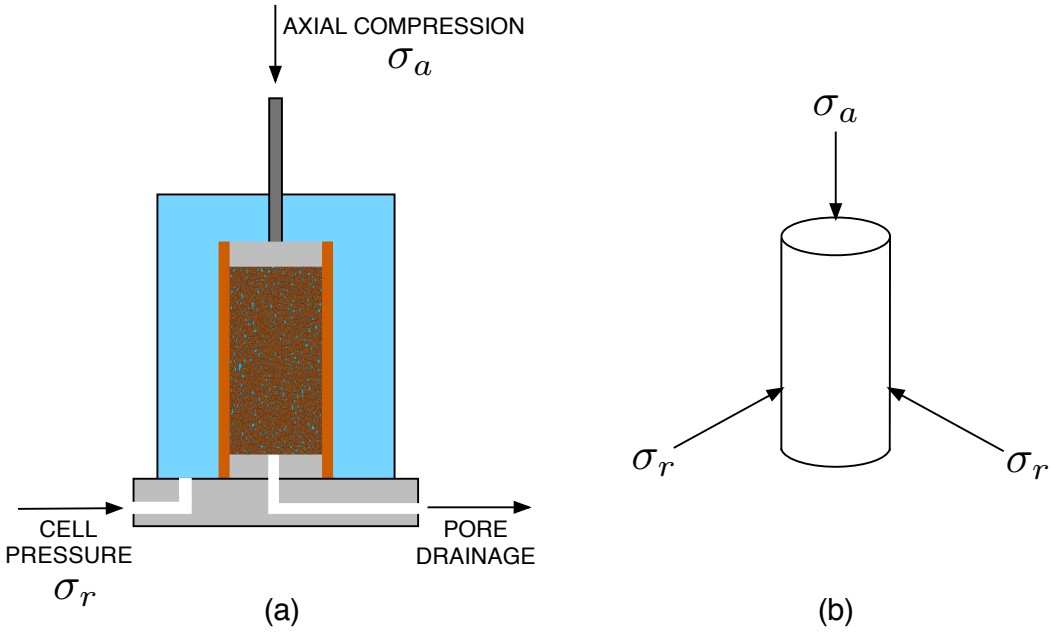

Figure 1.1: (a): Schematic diagram of the conventional triaxial test. (b): Imposed stress states

For the purpose of liquefaction testing, the specimen is first subjected to isotropic

consolidation under drained conditions. Thereafter, it is subjected to axial compression under undrained conditions. Figure 1.2 shows the stress paths obtained during static triaxial compression tests of loose and dense sands, under undrained conditions. Note that $q = (\sigma_a - \sigma_r)$ is the deviatoric stress, $p = (\sigma_a + 2\sigma_r)/3$ is the total volumetric stress, and p' is the effective volumetric stress. Total stresses are the stresses borne by the solid-fluid assembly, while effective stresses are the stresses borne only by the soil skeleton. Total and effective deviatoric stresses are the same, since the interstitial fluid is assumed to be incapable of providing shearing resistance.

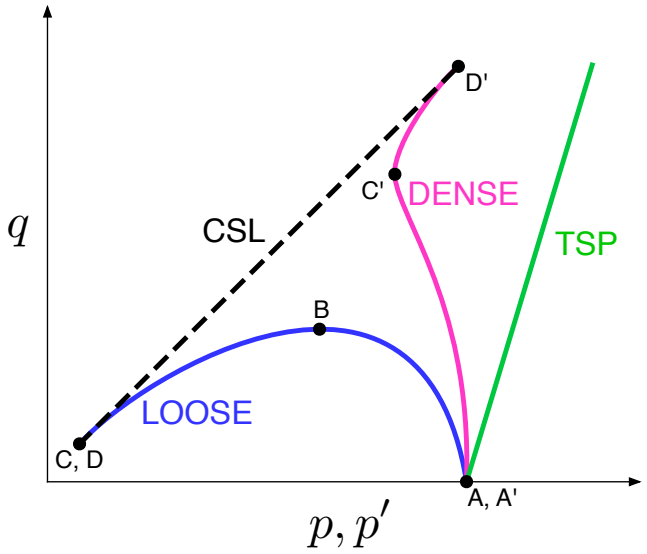

Figure 1.2: Effective stress paths of loose and dense sands under undrained triaxial compression. The total stress path (TSP) and critical state line (CSL) are also sketched for reference. A = start, B = Instability in loose sand, C & C' = phase transformation, D & D' = critical state. In loose sands, points C and D are often indistinguishable [36].

In the case of loose sands, the specimen undergoes a peak in stress space followed by a sudden collapse, accompanied by a large pore water pressure build up and extensive strain-softening. The peak in stress space is said to denote the onset of flow liquefaction instability [44]. On the other hand, dense sands are known to display a reversal in behavior - from contractive to dilative, during a phenomenon called 'phase transformation'. This phenomenon ostensibly provides stability to dense sands, whereby the pore water pressure build-up and strain softening are kept in check.

Conventionally, for static **slope stability analysis** under drained conditions, the stress state corresponding to the residual strength (or critical state) of the sand under drained loading is used as a measure of soil shear strength. For resistance to liquefaction, however, it has been suggested that the stress state corresponding to the peak (point B in Figure 1.2) in an undrained triaxial compression test should be used instead [32, 48]. Using analytical techniques like the 'method of slices' [16], or more advanced numerical techniques [28], the shear stress imposed on the soil can be calculated and compared with the soil strength to estimate a factor-of-safety.

(ii) Liquefaction charts

In order to evaluate liquefaction resistance of soils under dynamic or earthquake-induced loading, engineers often resort to liquefaction charts. Development of these charts involve (a) estimating stresses induced by an earthquake, and (b) estimating the strength of soils.

(a) Estimating stresses induced by an earthquake

Estimation of seismic demand on a soil element can be made via the 'simplified procedure', proposed by Seed and Idriss [71]. It is assumed that the seismic shear stresses induced at any depth in a soil deposit with a level ground surface are primarily due to the vertical propagation of horizontal shear waves. If the soil column above a soil element at depth h acted like a rigid body and the maximum ground surface acceleration were $a_{\max}$, the maximum shear stress $(\tau_{\max})_r$ on the soil element would be:

$$(\tau_{\max})_r = \frac{\gamma h}{g} a_{\max} = \sigma_v \frac{a_{\max}}{g} \tag{1.1}$$

where γ is the unit weight of the soil, and σ_v is the total vertical stress at depth h. See Figure 1.3. However, the soil column behaves like a deformable body, so the actual maximum shear stress $\tau_{\max}$ on the soil element would be:

$$\tau_{\max} = r_d (\tau_{\max})_r \tag{1.2}$$

where $r_d < 1$ is a stress reduction coefficient. $r_d = 1$ at the surface and decreases as the depth increases. Semi-empirical expressions exist for evaluating r_d up to a depth of 20 m [34, 88].

The cyclic stresses induced during an earthquake constitute an irregular time series with numerous cycles of different magnitudes. Studies have shown that an irregular

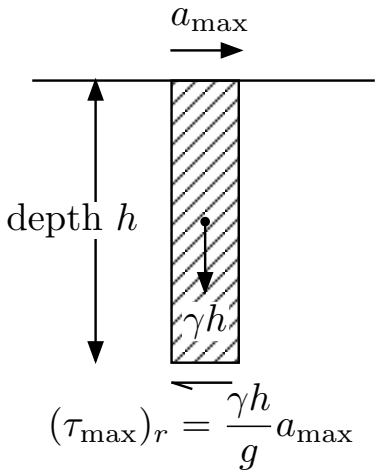

Figure 1.3: Maximum shear stress $(\tau_{\max})_r$ on a rigid block of sand at depth h from the surface.

time series can be approximated by a uniform cyclic stress time series with an equivalent number of uniform cycles [34, 70]. Seed and Idriss [71] arbitrarily chose a uniform average cyclic stress, τ_{avg} equal to 0.65 of the peak cyclic stress, $\tau_{\max}$. Hence:

$$\tau_{\text{avg}} = 0.65\, \sigma_v \frac{a_{\max}}{g} r_d \tag{1.3}$$

The number of uniform cycles N corresponding to τ_{avg} is semi-empirically related to earthquake magnitude [34, 70]. For instance, a magnitude 7.5 earthquake has been proposed to correspond to 15 cycles. The average cyclic stress is then normalized by the effective vertical confining pressure σ'_v to yield the cyclic stress ratio (CSR) imposed on a soil element at depth h by an earthquake:

$$\text{CSR} = \frac{\tau_{\text{avg}}}{\sigma'_v} = 0.65\, \frac{\sigma_v}{\sigma'_v} \frac{a_{\max}}{g} r_d \tag{1.4}$$

The seismic demand on a soil element is commonly expressed in terms of CSR. The CSR that is just sufficient to cause soil liquefaction is called the cyclic resistance ratio (CRR), and is a measure of the strength of soils. Determination of CRR is briefly reviewed next.

(b) Estimating strength of soils

Determination of in-situ CRR of sands can be done via laboratory testing of field samples [72]. The sample would be subjected to N cycles of cyclic loading, where N is empirically related to the earthquake magnitude. The uniform stress ratio (τ/σ'_v) that would cause liquefaction in N cycles would be recorded as CRR, and

then checked against CSR obtained in equation 1.4. If CRR exceeds CSR, the soil is stable. If not, it is susceptible to liquefaction. However, retrieval of soil specimens from the field using typical drilling and sampling techniques induces a lot of disturbance, making it difficult to translate laboratory test results onto field conditions. Therefore, semi-empirical relationships have been developed between CRR of sands and the results of in-situ tests (such as penetration tests and shear velocity measurements) by compiling case histories in which evidence of liquefaction had or had not been observed [34, 88].

Figure 1.4 illustrates a schematic of liquefaction charts. The abscissa plots soil properties as determined from in-situ tests, such as relative density, penetration resistance, and shear wave velocity. The ordinate plots the CSR. By plotting case histories on such a chart, it has been observed that cases of liquefaction and non-liquefaction could be roughly demarcated by a boundary. The boundary represents the in-situ CRR of sands.

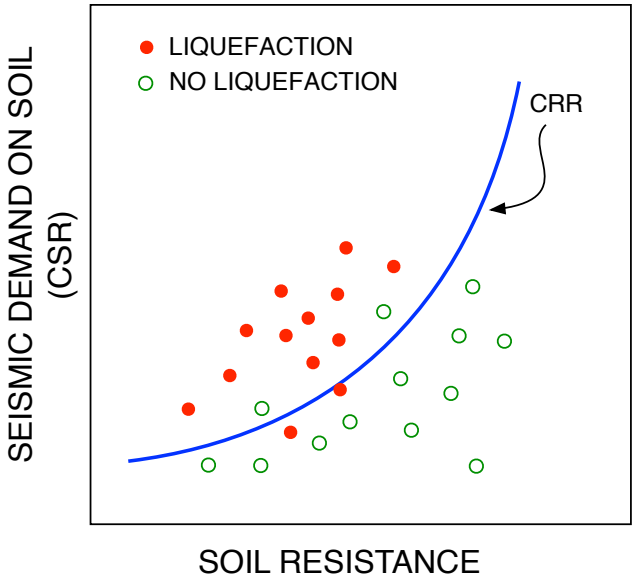

Figure 1.4: Schematic illustrating liquefaction charts. Liquefaction (solid red) and non-liquefaction (open green) case histories are plotted on a graph. Soil resistance can be in terms of relative density, penetration resistance, or shear wave velocity. The two types of case histories can be roughly demarcated by a boundary, which denotes the in-situ CRR of sands.

1.3 Research Objectives

We are now in a position to outline our research objectives. It can be appreciated that liquefaction poses a significant risk to distributed infrastructure systems that are vital for the security, economy, safety, health, and welfare of societies. In order to make our cities more resilient to the effects of liquefaction, it is important to be able to identify areas that are most susceptible. As discussed, conventional slope stability analysis and the use of liquefaction charts help in that endeavor. However, these methodologies have some limitations, which motivate the research objectives for this dissertation.

For instance, liquefaction charts are compiled using case histories, which make them inherently empirical. This limits their scope of application. To reliably extend their scope, high-quality field data are needed. However, field data can only be obtained following earthquake-induced liquefaction. Therefore, it is important to incorporate physics in these charts, so that they can make reliable predictions in the absence of sufficient field data. The first step in that endeavor is to develop a deeper understanding of the fundamental physics of soil liquefaction.

Furthermore, liquefaction charts can only determine the liquefaction susceptibility of a site. They do not inform us about the effects of liquefaction. If a site will liquefy, will it experience flow liquefaction or cyclic mobility? In other words, will liquefaction cause only a slight settlement of foundations or will it cause entire buildings to topple? Liquefaction charts do not make these distinctions. Such information is crucial when it comes to evaluating surface hazards of liquefaction, necessitating a more physical understanding of these charts.

Conventional slope stability analysis assumes that soil will fail under drained conditions, via strain-localization. However, locally undrained conditions can make the slope susceptible to static liquefaction [32, 48]. This contrast in soil behavior due to different drainage conditions poses some questions. For instance, although a dense sand is stable under undrained loading, what happens under partial drainage conditions? How do we estimate the soil strength in that case? Such questions necessitate further research into the subject of static liquefaction.

The most fundamental way to measure soil strength is via laboratory testing. How-

ever, retrieval of soil specimens from the field using typical drilling and sampling techniques induces a lot of disturbance, which alters the mechanical properties of soil. As a result, in-situ testing techniques have gained prominence. The discrepancy in mechanical behavior is often attributed to the difference in soil fabric, or grain arrangement, of laboratory soil sample and in-situ soil [34, 70]. In principle, if we can quantify the soil fabric in the laboratory and in-situ, it may be possible to translate laboratory test results to field conditions. However, fabric quantification measures [45] need grain-scale information, making them impractical for quantification of in-situ fabric. This raises a fundamental question – is it possible to quantify in-situ soil fabric at all? If so, how? These are important questions, seeking answers to which require further research.

1.4 Scope of Thesis

The thesis is organized as follows. Chapter 2 focuses on developing a deeper understanding of the fundamental physics of soil liquefaction. This is achieved by investigating what is perhaps the simplest manifestation of liquefaction, namely static loading in a triaxial compression test. Specifically, the chapter addresses the mechanics of origin of flow liquefaction instability in a triaxial compression test, under static, or monotonic loading. It defines a flow liquefaction potential that helps understand why certain soils liquefy under certain conditions. It also proposes a necessary precursor, or warning sign, prior to the onset of flow liquefaction. The validity of the flow liquefaction potential and necessary precursor were checked using discrete element method simulations [17].

Chapter 3 numerically investigates the mechanics of liquefaction charts, and proposes flow liquefaction as a mechanism for the lower end of these charts. This yields a more physical understanding of such charts and can provide an engineer additional information regarding the effects of liquefaction. The numerical tool employed was the Dafalias-Manzari model [18], which is a continuum plasticity model.

Chapter 4 investigates the effect of fabric on shear wave velocity V_S in soils. As mentioned in section 1.2, V_S is one of the indices that are used for quantifying soil resistance to liquefaction. In essence, it acts as a proxy for parameters affecting soil behavior, such as relative density and confining stress. By understanding how

fabric affects V_S, V_S may also be able to act as a proxy for soil fabric, and help in quantification of in-situ soil fabric. Quantification of in-situ soil fabric may enable investigators to translate laboratory test results on to field conditions, with greater certainty. This investigation was numerically performed using the level sets discrete element method [39, 41].

Finally, Chapter 5 summarizes some key developments of this dissertation.

Chapters 2, 3, and 4 can be read independently. Chapter 2 is a published article [58], while Chapters 3 and 4 have been submitted [59, 60] to journals for possible publication. Due to the independent nature of these chapters, there is invariably some content repetition.